Available online at www.sciencedirect.com

ScienceDirect

Procedia Engineering 4 (2010) 243–251

Procedia Engineering

www.elsevier.com/locate/procedia

ISAB-2010

Slack phenomena in tethers of submerged floating tunnels under hydrodynamic loads

Wei Lu, Fei Ge, Lei Wang, Youshi Hong*

State Key Laboratory of Nonlinear Mechanics, Institute of Mechanics, Chinese Academy of Sciences, 15 Beisihuanxi Rd, Beijing100190, China

Received 16 July 2010; revised 2 August 2010; accepted 3 August 2010

Abstract

The tethers of submerged floating tunnels (SFT) might undergo slack in some serve sea states. It is one of the possible hazard conditions SFT confronted. This paper investigates the slack phenomena in SFT tethers under hydrodynamic loads. A bilinear stiffness model is used to simulate SFT tethers. Results show that the tether will go slack under a large wave height and snap force happens. The occurrence of the current makes the tethers downstream prone to slack. Then a procedure for preliminary slack prediction is introduced. Slack criterion and an analytical solution of SFT pre-slacking response is derived for the prediction. The procedure provides a practical method for selection of the design values of SFT structure configurations.

Keywords: submerged floating tunnels; slack phenomena; bilinear stiffness; hydrodynamic loads; slack prediction; structure configuration

1. Introduction

Submerged floating tunnels (SFT) i.e. Archimedes Bridge is an innovative transportation technology for crossing straits, lakes, or other water sounds. It is tube like structure floating at certain depth in the water which takes the advantage of buoyancy and is tethered to the foundation and the shores [1]-[2]. With its economical and environmental advantages, it has become one of the most promising alternatives for water crossings. To realize such a structure, many problems of science and technology are still to be solved, such as fluid-structure-soil coupling, vortex induced vibration of tethers, the architecture design of the tunnel, the configuration of cable systems, the tunnel-shore joint design, etc. [3]. Many researches have been carried out in the aspects of conceptual design and dynamic response by investigators from Italy, Norway, Japan, China and USA, etc. [4].

For the type of SFT moored by tethers, slack in one or more tethers could be one of the most critical conditions that may be encountered. The occurrence of this phenomenon is due to the fact that the tether is highly resistible to tension while could hardly undertake compression. The slack of tether might induce the temporary dynamic instability of SFT for loss of restraint. Besides, when the tether transits alternatively between the states of slack and

* Corresponding author. Tel.: 86-10-82543968; fax: 86-10-62561284.
E-mail address: hongys@imech.ac.cn

1877-7058 © 2010 Elsevier Ltd. Open access under CC BY-NC-ND license.
doi:10.1016/j.proeng.2010.08.028

taut, the instant tension force of a large value might occur which is referred as the 'snap force' [5]. It might cause a sudden breakage of SFT tether.

The necessity of the research of SFT tether slacking lies in two aspects mainly: for one aspect, on the design stage the structure configuration should be chosen to avoid the occurrence of tether slacking under the specified local load conditions; for another aspect, as a matter of fact, it could hardly prevent the occurrence of tether slacking in some severe conditions for the unpredictability of all kinds of disasters. Accordingly, special attentions are paid to: of what structure design configurations the tether would become slack; how will SFT behave if tether slacks.

In this paper, a bilinear stiffness model is used to simulate the mooring tether of SFT, and both pre- and post-slacking behaviours under hydrodynamic loading are obtained. Then practical procedure was introduced to select the design values of SFT structure configurations on consideration of preventing tether slacking by deriving the slack criterion and analytical solution to SFT pre-slacking response.

2. Governing equations

The conceptual design of Funka Bay SFT with a four tether moored type is taken as the analysis case in this paper [6]. It has a main body with four car lanes and two railway lanes. The detailed structure configurations and fluid environmental conditions are listed in Table 1.

A single tunnel segment is considered as showed in Fig. 1. When modeling the tunnel is considered as rigid; the fluid force is supposed to perpendicular to the axis of the tunnel; the tether is assumed to be of material linearity. A bilinear stiffness model is used to simulate SFT tethers. When tether is taut the tensile stiffness remains constant as k. When the tether goes slack, the stiffness becomes zero. It can be expressed as:

$$K_{\mathrm{i}}(\Delta L_{\mathrm{i}})=\begin{cases} k & (\Delta L_{\mathrm{i}}\geq 0) \\ 0 & (\Delta L_{\mathrm{i}}<0) \end{cases},\ \Delta L_{\mathrm{i}}=L_{\mathrm{i}}-L_n \quad \mathrm{i}=1\ldots 4 \tag{1}$$

where L_{i} is the instant length of the i-th tether, L_n is the unstrained length. Lagrange equation is used to derive the equation. The governing equations can be expressed as:

$$\begin{cases} m\ddot{x}+\dfrac{1}{2}\displaystyle\sum_{\mathrm{i}=1}^{4}K_{\mathrm{i}}(\Delta L_{\mathrm{i}})\frac{\partial(\Delta L_{\mathrm{i}}^{2})}{\partial x}=f_x a \\ m\ddot{y}-\left(w-\dfrac{1}{2}\displaystyle\sum_{\mathrm{i}=1}^{4}K_{\mathrm{i}}(\Delta L_{\mathrm{i}})\frac{\partial(\Delta L_{\mathrm{i}}^{2})}{\partial y}\right)=f_y a \\ \dfrac{1}{2}mR^{2}\ddot{\varphi}+\dfrac{1}{2}\displaystyle\sum_{\mathrm{i}=1}^{4}K_{\mathrm{i}}(\Delta L_{\mathrm{i}})\frac{\partial(\Delta L_{\mathrm{i}}^{2})}{\partial \varphi}=f_\varphi a \end{cases} \tag{2}$$

where m is the mass of the tunnel segment, R is the outer radius of the tunnel, and x, y, φ denotes the displacement in x, y direction and rotation angle about the tunnel axis.

Table 1. Structure parameters and fluid environmental conditions of Funka Bay SFT

Structural properties	Symbol	Value	Fluid dynamic environment	Symbol	Value
Total tunnel length	L_{t}	30 km	Water depth	d	100 m
Length of single tunnel module	a	93.2 m	Significant wave height	H_s	9.3 m
Tunnel submerged depth (from centre)	e	41.5 m	Wave period	T	13 s
Tunnel outer diameter	D	23 m	Current velocity	V_c	0.6 m/s
Connection angle	ψ_0	30°	Drag coefficient	C_D	1.0
Tether tensile stiffness	k	3.6×10^{8} N/m	Added-mass coefficient	C_M	1.0

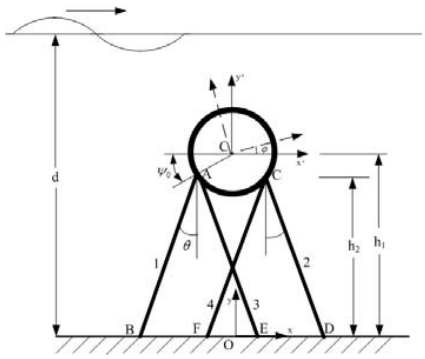

Fig.1. Sketch of SFT cross section

Generally there are three different ways to calculate the wave forces: Morison equation, Froude-Krylov theory and diffraction theory. When the ratio of tunnel outer diameter D to wave length λ is smaller than 0.2 as the present case is, the present of SFT is with little influence on the propagation of the surface wave, and Morison equation validates. The fluid force in each direction f_x, f_y, f_φ is written as:

$$f_x = \rho_{\mathrm{w}} \mathrm{A}\dot{w}_x + C_{\mathrm{M}}\rho_{\mathrm{w}}\mathrm{A}(\dot{w}_x + V_c - \ddot{x}) + \frac{1}{2}\rho_{\mathrm{w}} D C_{\mathrm{D}} \left|w_x + V_c - \dot{x}\right|(w_x - \dot{x}) \tag{3}$$

$$f_y = \rho_{\mathrm{w}} \mathrm{A}\dot{w}_y + C_{\mathrm{M}}\rho_{\mathrm{w}}\mathrm{A}(\dot{w}_y - \ddot{y}) + \frac{1}{2}\rho_{\mathrm{w}} D C_{\mathrm{D}} \left|w_y - \dot{y}\right|(w_y - \dot{y}) \tag{4}$$

$f_\varphi = 0$ (The wave force is assumed to exert on the centre of tunnel cross section.) *(5)*

where ρ_{w} is the density of the fluid, A is the cross section area of SFT, and w_x, w_y are respectively velocity of water particles in x, y direction each.

3. Comparison of wave theories

The region of application of different wave theories depends on two normalized parameters, H/T^2 and d/T^2. In present case researched, when the wave height is small (not greater than 1m) it lies in the valid region of Airy wave theory; otherwise it lies in the region of Stokes wave theory [7]. In this part, comparison of Airy wave theory and Stokes fifth order wave theory is made. Results indicate that for SFT, Airy wave theory is also feasible even for a large wave height.

Take a regular wave with a height of 9m and a period of 13s as example, Fig. 2a and 2b gives the velocity distributions of horizontal and vertical water particles respectively. The difference of the two theories is apparent only in area near the water surface. Fig. 3a and 3b gives the wave forces that SFT of different submerged depth undertakes in horizontal and vertical direction respectively. As one of the typical characters of SFT, enough submerged depth (usually 30m from top) is assured. Fig. 3a and 3b indicate that the difference of wave forces calculated by the two theories is subtle for SFT. It can be seen that Airy wave theory can provide a good precision. Besides, as the simplicity of Airy wave theory, it is taken in this paper.

4. Characteristics of SFT dynamic behavior when tether slacking

In this part, the fourth order Runge-Kutta method is used to solve the nonlinear governing Eqs. (2). The state of static equilibrium is taken as the initial conditions: $x(0) = 0, y(0) = h_1, \varphi(0) = 0$; $\dot{x}(0) = 0, \dot{y}(0) = 0, \dot{\varphi}(0) = 0$.

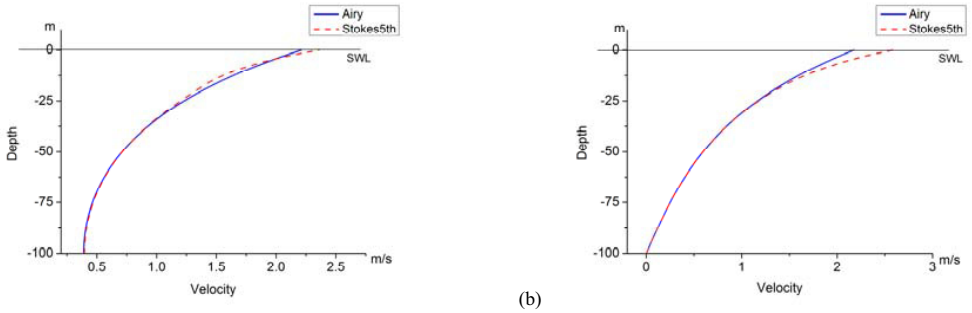

Fig. 2. Distribution of velocity of water particles: (a) Horizontal; (b) Vertical (wave height: 9m, wave period: 13s)

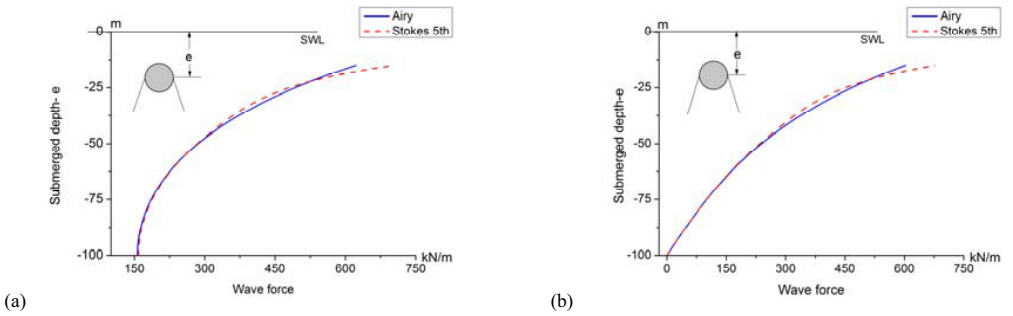

Fig. 3. Wave forces on SFT of different submerged depth: (a) Horizontal; (b) Vertical (wave height: 9m, wave period: 13s)

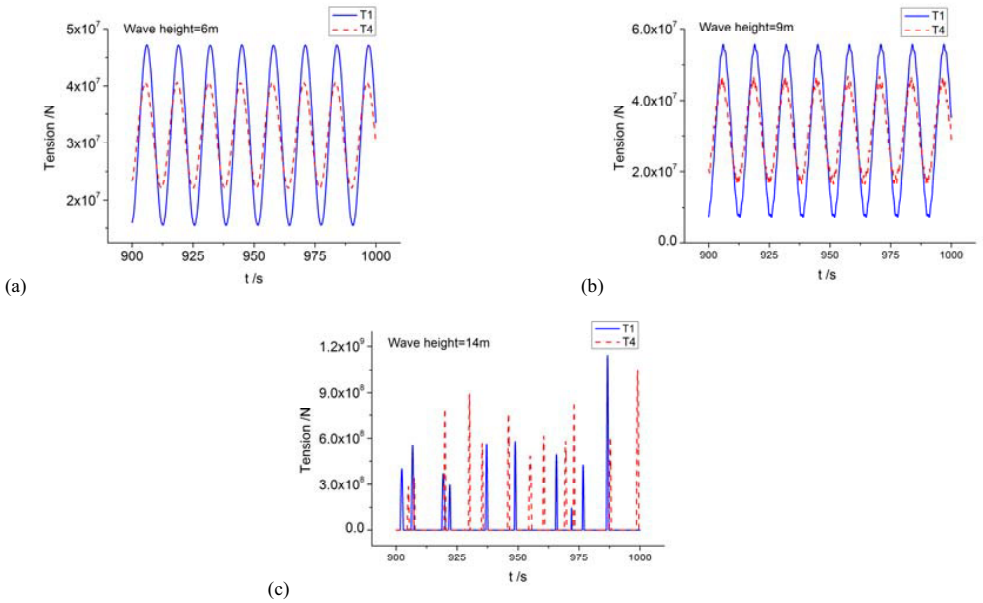

Fig. 4. Dynamic tension force of SFT tethers under different wave heights (wave period: 13s): (a) Wave height: 6m; (b) Wave height: 9m; (c) Wave height: 14m

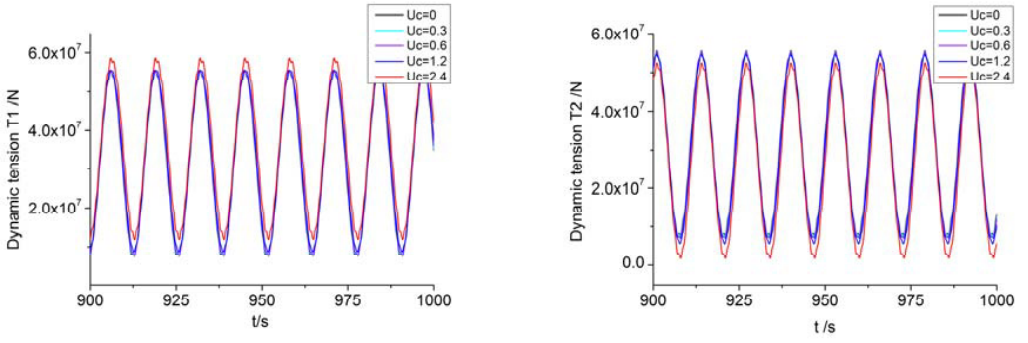

Fig. 5. Dynamic tension force of SFT with coexistence of wave and current (Wave height: 9m; Wave Period: 13s): (a) Tension of upstream tether T1; (b) Tension of downstream tether T2

The structure configuration with a mooring angle of 30° and a buoyancy-weight-ratio of 1.4 is taken as the example to illustrate the characteristics both of SFT pre- and post-slacking dynamic behavior. Fig. 4a and 4b and 4c gives the dynamic tension responses of SFT tethers under different wave conditions. When the wave height is as small as 6m, the dynamic response of tether tension force is harmonic. When the wave height increase as large as 9m, the response of tether tension force is no longer harmonic, but still is periodic. When the wave height is as large as 14m, the tether will go slack, and the tension force reaches its peak in a short time and then drops. The so called "snap force" occurs.

The cases with the coexistence of wave and current are also considered. As showed in Fig. 5, when there is the coexistence of current, the mean value of the tension of upstream tethers will become larger as the current velocity increases; while the mean value of downstream tether tension will become smaller. The downstream tethers are more prone to go slack with the existence of current. However, under the wave condition considered in this case, slack in the tether does not happen despite of a significant current velocity.

5. Practical procedure for preliminary slack prediction

By the aforementioned method of solving the nonlinear governing equations of SFT numerically, the dynamic responses of both pre- and post-slacking behavior of SFT can be obtained. With running more cases, one can make slack predictions under given conditions. However, it is time consuming. In this part, a simple method for a practical procedure to make preliminary slack prediction is introduced.

In fact the pre-slacking response is sufficient to decide whether SFT tether will go slack or not. In this light, two assumptions are made in this part: a linear tensile stiffness, i.e. $K_i = k$; a small rotation angle, which means neglecting the rotation i.e. $\varphi(t) = 0$. Based on these assumptions, slack criterion is firstly built and then the analytical solution of the pre-slacking dynamic response of SFT is pursued to make slack prediction. Two fundamental structural parameters, mooring angle and buoyancy-weight-ratio (BWR) are chosen as the target design parameters for SFT structure configuration.

5.1. Slack criterion

With the assumption of small rotation, there are the following relations: $L_1(t) = L_4(t)$, $L_2(t) = L_3(t)$. If SFT tethers do not go slack, $L_1(t) \geq L_n$ and $L_2(t) \geq L_n$ must be satisfied simultaneously. Expand the expression of $L_1(t)$ and $L_2(t)$ so that slack criterion is given by the following inequalities：

$$\begin{cases} (x + h_2 \tan\theta)^2 + (\delta y + h_2)^2 \geq \left(\dfrac{h_2}{\cos\theta + \dfrac{w}{4EA}} \right)^2 \\ (x - h_2 \tan\theta)^2 + (\delta y + h_2)^2 \geq \left(\dfrac{h_2}{\cos\theta + \dfrac{w}{4EA}} \right)^2 \end{cases} \tag{6}$$

in which $\delta y = y - h_1$.

In coordinate with x as its abscissa and δy as its ordinate, slack region is the total area of the two circles which is the shadow region as showed in Fig. 6.

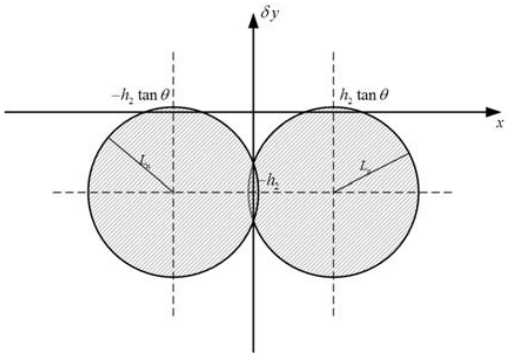

Fig. 6. Slack region of SFT

5.2. Linearization of governing equation

The governing equations are simplified as following with the aforementioned assumption in this part:

$$\begin{cases} \dfrac{m}{a}\ddot{x} + \dfrac{1}{2}\sum_{i=1}^{4} \dfrac{K_i(\Delta L_i)}{a} \dfrac{\partial(\Delta L_i^2)}{\partial x} = f_x \\ \dfrac{m}{a}\ddot{y} - \left(\dfrac{w}{a} - \dfrac{1}{2}\sum_{i=1}^{4} \dfrac{K_i(\Delta L_i)}{a} \dfrac{\partial(\Delta L_i^2)}{\partial y} \right) = f_y \end{cases} \tag{7}$$

Only fluid force induced by wave is considered in this part, and linearization of the wave force and resorting force are made. To simplify the drag term of fluid force, structure velocity is assumed to be small with reference to water velocity so that the fluid force can be written as [8]:

$$f_x \cong (C_M + 1)\rho_w A \dot{w}_x - C_M \rho_w A \ddot{x} + \bar{C}_D w_x - 2\bar{C}_D \dot{x} \tag{8}$$

A similar simplification is made to f_y.

On the other hand, the resorting forces can be linearized by assuming a small structure displacement and a constant tensile stiffness of tethers.

$$\frac{1}{2}\sum_{i=1}^{4}\frac{K_i(\Delta L_i)}{a}\frac{\partial(\Delta L_i^2)}{\partial x}\cong K_x x \tag{9}$$

$$\frac{1}{2}\sum_{i=1}^{4}\frac{K_i(\Delta L_i)}{a}\frac{\partial(\Delta L_i^2)}{\partial y}\cong K_y \delta y + C_y \tag{10}$$

By using Eqs. (8)-(10), the simplified governing Eqs. (7) can be written as:

$$\begin{cases} \ddot{x}+2\xi_x\omega_x\dot{x}+\omega_x^2 x=\frac{\alpha_x}{m^*}\sin(\omega t+\varphi_x) \\ (\ddot{\delta y})+2\xi_y\omega_y(\dot{\delta y})+\omega_y^2\delta y=-\frac{\alpha_y}{m^*}\sin(\omega t+\varphi_y) \end{cases} \tag{11}$$

The detailed form of the coefficient in *(8)-(11)* is attached to Appendix A. The analytical steady solutions to these linear equations are:

$$\begin{cases} x_p(t)=\rho_x\sin(\omega t+\varphi_x-\theta_x).\ \rho_x=\frac{\alpha_x}{K_x}[(1-\beta_x^2)^2+(2\xi_x\beta_x)^2]^{-1/2};\theta_x=\arctan(\frac{2\xi_x\beta_x}{1-\beta_x^2});\quad \beta_x=\frac{\omega}{\omega_x}. \\ \delta y_p(t)=-\rho_y\sin(\omega t+\varphi_y-\theta_y).\ \rho_y=\frac{\alpha_y}{K_y}[(1-\beta_y^2)^2+(2\xi_y\beta_y)^2]^{-1/2};\theta_y=\arctan(\frac{2\xi_y\beta_y}{1-\beta_y^2});\beta_y=\frac{\omega}{\omega_y} \end{cases} \tag{12}$$

Expressions (11) give the closed form of SFT non-slacking steady state solution. As long as it don not satisfy the slack criterion given by inequalities (6), the tether will go slack, and in that case the non-slacking solution invalidates.

Fig. 7 gives the critical wave height when tethers of SFT of different combinations of BWR and mooring angle go slack. Fig. 8 gives the relation of critical wave height with the mooring angle of four BWRs. When design, the structure configuration with combinations of the two target parameters of which the critical wave height is smaller than the designed wave height, should be avoided from the viewpoint of no slacking in tethers.

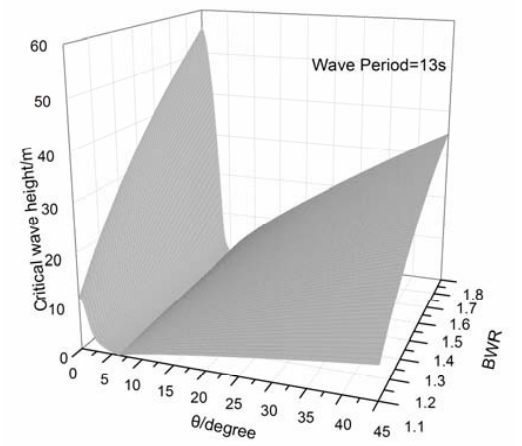

Fig. 7. Critical wave height of different combinations of BWR and mooring angle

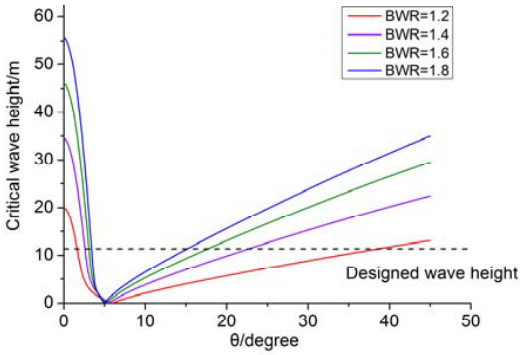

Fig. 8. Critical wave height vs. mooring angle of four BWRs

6. Conclusions

Slack in tethers is one of the most critical conditions that SFT may be encountered. It should be one of the major considerations when design. A bilinear stiffness model is used to simulate SFT tether. As certain submerged depth is generally assured for SFT, Airy linear wave theory can provide a good precision for calculating the water kinematics. Both of the pre- and post-slacking dynamic behavior is obtained. When the wave height is as large as 14m, the tether of SFT with a mooring angle of 30° and a BWR of 1.4 will go slack, and snap force happens. The occurrence of the current makes the tethers downstream prone to slack. A preliminary and fast prediction can be made by the practical procedure in Section 5. When design, the critical wave height of the target structure parameters should be larger than the designed wave height.

Acknowledgements

This paper is supported by National Natural Science Foundation of China (Grant nos. 10532070, 10772178) and Knowledge Innovation Program of Chinese Academy of Sciences (Grant no. KJCX2-YW-L07).

References

[1] Hong Y, Ge F, Long X. Researches on essential mechanics issues for submerged floating tunnel. *Proc. of the 5th symposium on strait crossings*; 2009, p. 251-256.

[2] FEHRL report no 1996/2a. *Analysis of the Submerged FloatingTtunnel Concept. FEHRL* (Forum of European National Highway Research Laboratories). Berkshire (Crowthorne): Transport Research Laboratory; 1996.

[3] Huang GJ, Wu YX, Hong YS. Transportation of crossing waterways via Archimedes Bridge. *Shipbuilding of China* 2002; 43(S): 13–18.

[4] Dong M, Ge F, Hui L, Hong YS. Research progress in submerged floating tunnels. *China J Highway Transport* 2007; 20: 101-107.

[5] Niedzwecki JM, Thampi SK. Snap loading of marine cable systems. *Applied Ocean Research* 1991; 13(1): 2–11.

[6] Maeda N, Morikawa M, Ishikawa K, Kakuta Y. Study on structural characteristics of support systems for submerged floating tunnel. *Proc. of the 3rd symposium on strait crossings*; 1994, p. 579-674.

[7] Chakrabarti SK. *Hydrodynamics of offshore structures*. Boston: Computation Mechanics Publications; 1987.

[8] Fogazzi P and Perotti F. The dynamic response of seabed anchored floating tunnels under seismic excitation. *Earthquake engineering and structural dynamics* 2000; 29: 273–295.

Appendix A.

The detailed expression of the coefficients in expressions and equations (8)-(12) is given here.

$$\overline{C}_D = \frac{1}{2}\rho_w D C_D \hat{w}_x$$

$$\hat{w}_x = \frac{8}{3\pi}\frac{\omega H}{2}\frac{\cosh(ky)}{\sinh(kd)}$$

$$K_x = \frac{4K}{a}\left[1+\frac{(h_2\tan\theta)^2 L_n}{(h_2\sec\theta)^3}-\frac{L_n}{h_2\sec\theta}\right]$$

$$K_y = \frac{4K}{a}\left[1+\frac{h_2{}^2 L_n}{(h_2\sec\theta)^3}-\frac{L_n}{h_2\sec\theta}\right]$$

$$C_y = \frac{4K}{a}\left(h_2 - L_n\cos\theta\right) = \frac{w}{a}$$

$$m^* = m/a + C_M\rho_w A$$

$$\alpha_x = \frac{\cosh(kh_1)}{\sinh(kd)}\sqrt{\left(\overline{C}_D\frac{\pi H}{T}\right)^2+\left[(C_M+1)\rho_w A\frac{2\pi^2 H}{T^2}\right]^2}$$

$$\tan\varphi_x = -\frac{\overline{C}_D T}{2\pi\rho_w A\left(C_M+1\right)}$$

$$\alpha_y = \frac{\sinh(kh_1)}{\sinh(kd)}\sqrt{\left(\overline{C}_D\frac{\pi H}{T}\right)^2+\left[(C_M+1)\rho_w A\frac{2\pi^2 H}{T^2}\right]^2}$$

$$\varphi_y = \varphi_x + \frac{\pi}{2}.$$